

# Major mutations in calf-1 and calf-2 domains of glycoprotein IIb in patients with Glanzmann thrombasthenia enable GPIIb/IIIa complex formation, but impair its transport from the endoplasmic reticulum to the Golgi apparatus

Nurit Rosenberg, Rivka Yatuv, Vladimir Sobolev, Hava Peretz, Ariella Zivelin, and Uri Seligsohn

The crystal structure of integrin  $\alpha_v\beta_3$  comprises 3 regions of contact between  $\alpha_v$  and  $\beta_3$ . The main contact on  $\alpha_v$  is located in the  $\beta$ -propeller while calf-1 and calf-2 domains contribute minor interfaces. Whether or not contacts between calf-1 and calf-2 domains of glycoprotein (GP) IIb ( $\alpha$ IIb) and GPIIIa ( $\beta$ 3) play a role in GPIIb/IIIa complex formation has not been established. In this study we analyzed the effects of 2 naturally occurring mutations in calf-1 and calf-2 domains on GPIIb/IIIa complex formation, its processing, and transport to the cell membrane. The mutations investigated were a deletion-insertion

in exon 25 located in calf-2 and an in-frame skipping of exon 20 located in calf-1. Mutated GPIIb cDNAs were co-transfected in baby hamster kidney cells with normal GPIIIa ( $\beta$ 3) cDNA. Analysis by flow cytometry failed to demonstrate detectable amounts of GPIIb or GPIIb/IIIa complex on the surface of cells transfected with each mutation, but immunohistochemical staining revealed their intracellular presence. GPIIb was mainly demonstrable as pro-GPIIb by immunoprecipitation of cell lysates expressing each mutation. Differential immunofluorescence staining of GPIIb and cellular organelles suggested that most altered

complexes were located in the endoplasmic reticulum. Homology modeling of normal GPIIb based on the  $\alpha_v\beta_3$  crystal structure revealed similar contacts between  $\alpha_v$  and  $\beta_3$  and between  $\alpha$ IIb and  $\beta$ 3. Introduction of the mutations into the model yielded partial disruption of the normal contacts in the corresponding domains. These data suggest that despite partial disruption of calf-1 or calf-2 domain, GPIIb/IIIa complex is formed but its transport from the endoplasmic reticulum is impaired. (Blood. 2003;101:4808-4815)

© 2003 by The American Society of Hematology

## Introduction

Platelet aggregation depends on fibrinogen binding to glycoprotein (GP) IIb/IIIa complex ( $\alpha$ IIb $\beta$ 3), which is a calcium-dependent heterodimer expressed exclusively in megakaryocytes and platelets.<sup>1</sup> GPIIb and GPIIIa are encoded by separate genes, and following their synthesis they are introduced into the endoplasmic reticulum (ER) where they undergo N-linked glycosylation, form disulfide bonds, and assemble in GPIIb/IIIa complexes. The complex is then transported to the Golgi apparatus for final oligosaccharide processing and cleavage of single-chain pro-GPIIb into mature GPIIb, comprising a heavy and light chain. From the Golgi apparatus the complex is transported to the open canalicular system and then to the  $\alpha$  granules or plasma membrane.<sup>2,3</sup> The assembly of GPIIb and GPIIIa as a complex is a prerequisite for its surface expression.<sup>3</sup>

A diminished amount or dysfunction of the GPIIb/IIIa complex causes Glanzmann thrombasthenia (GT). GT is transmitted in an autosomal recessive manner and is caused by mutations in either GPIIb or GPIIIa genes.<sup>4</sup> So far more than 60 mutations causing GT have been described and listed in a database.<sup>5</sup> Expression of some of these mutations in heterologous cell cultures has shed light on the functional importance of particular domains within GPIIb and GPIIIa in the assembly of GPIIb/IIIa complex. Similar information

has also been derived from immunochemical analyses of soluble GPIIb/IIIa complex and from the crystal structure of soluble  $\alpha_v\beta_3$ , which is closely related to  $\alpha$ IIb $\beta$ 3.<sup>6,7</sup> By immunochemical examinations it was demonstrated that the C-terminal region of GPIIb, including parts of calf-1 and calf-2 domains, is involved in the contact between GPIIb and GPIIIa.<sup>6</sup> The crystal structure of the extracellular part of integrin  $\alpha_v\beta_3$  revealed that while the main contact between  $\alpha_v$  and  $\beta_3$  lies in the  $\beta$ -propeller of  $\alpha_v$  and  $\beta$ A domain of  $\beta_3$ , additional contacts between calf-1 and calf-2 domains of  $\alpha_v$  and epidermal growth factor (EGF)-3, EGF-4, and  $\beta$  tail domain ( $\beta$ TD) domains of  $\beta_3$  were also depicted. The latter contacts were small and discontinuous and therefore believed not to occur in the membrane-bound receptor.<sup>7</sup> This apparent weakness of the contacts could also be inferred from an electron microscopy study that demonstrated that GPIIb/IIIa complexes had a globular head with 2 flexible tails that were sometimes joined together and sometimes spread apart.<sup>8</sup> However, a recent electron microscopy study that included physicochemical measurements of normal and mutated  $\alpha_v\beta_3$  and  $\alpha$ IIb $\beta$ 3 demonstrated that in the low-affinity state, in solution, and on cell surface, the tails of the  $\alpha$  and  $\beta$  subunits have substantial interactions with one another.<sup>9</sup> This study also showed that activation of  $\alpha_v\beta_3$  resulted in a dramatic

From the Thrombosis and Hemostasis Research Institute, The Chaim Sheba Medical Center, Tel-Hashomer; Sackler Faculty of Medicine, Tel Aviv University; and Department of Plant Sciences, Weizmann Institute of Science, Rehovot, Israel.

Submitted August 12, 2002; accepted February 9, 2003. Prepublished online as *Blood* First Edition Paper, February 27, 2003; DOI 10.1182/blood-2002-08-2452.

Supported by the Israeli Science Foundation administrated by the Israel

Academy of Sciences and Humanities.

**Reprints:** Uri Seligsohn, Institute of Thrombosis and Hemostasis, Sheba Medical Center, Tel-Hashomer, Israel; e-mail: zeligson@post.tau.ac.il and seligson@sheba.health.gov.il.

The publication costs of this article were defrayed in part by page charge payment. Therefore, and solely to indicate this fact, this article is hereby marked "advertisement" in accordance with 18 U.S.C. section 1734.

© 2003 by The American Society of Hematology

rearrangement to an extended conformation in which no association between the tails of the  $\alpha$  and  $\beta$  subunits was displayed.<sup>9</sup>

We have previously described 2 major mutations in the calf-1 and calf-2 domains of the GPIIb gene in patients with GT. One mutation in calf-2, a 6-bp deletion and 31-bp insertion in exon 25, leads to cryptic splicing of exon 25 and results in substitution of Leu786-Asn795 (LHNNPGTVN) by 8 alternative amino acids (GLHLSIHQ).<sup>10</sup> A second mutation in calf-1, an A→G transition in the acceptor splice site of intron 19–exon 20 junction, results in 4 alternatively spliced mRNAs, all lacking exon 20 with 3 of them remaining in-frame.<sup>11</sup> In an attempt to clarify the importance of the contact between calf-1 and calf-2 of GPIIb and EGF-3, EGF-4, and  $\beta$ TD of GPIIIa, we analyzed the effects of these major mutations in calf-1 and calf-2 on GPIIb/IIIa complex formation, its processing, and transport to the cell membrane.

## Materials and methods

### Antibodies

A rabbit polyclonal antibody recognizing both reduced GPIIb and nonreduced GPIIIa was previously produced in our laboratory.<sup>12</sup> Murine monoclonal antibodies, AP3 specific for GPIIIa and AP2 specific for GPIIb/IIIa complex, were generously provided by Dr Thomas Kunicki from Scripps Research Institute (La Jolla, CA), and monoclonal antibody 10E5 specific for GPIIb/IIIa complex was a gift from Dr Barry Collier from Rockefeller University, New York, NY. Murine monoclonal antibodies SZ22 against the heavy chain of GPIIb and P2 recognizing GPIIb only when complexed with GPIIIa were purchased from Immunotech (Marseille, France). Monoclonal antibody CA3 against human GPIIb and polyclonal rabbit antihuman- $\beta$ 3 antibody were purchased from Chemicon International (Temecula, CA). Rabbit antirat mannosidase II antiserum was purchased from Dr Kelley W. Moremen, University of Georgia, Athens, and rabbit anticanine calnexin carboxyl terminus was purchased from Stressgene Biotechnologies (Victoria, BC, Canada). Goat antimouse immunoglobulin G (IgG) fluorescein isothiocyanate (FITC) conjugate, goat antimouse IgG agarose conjugate, goat antimouse peroxidase conjugate, goat antirabbit IgG agarose conjugate, and goat antirabbit IgG peroxidase were purchased from Sigma (St Louis, MO). Goat antirabbit IgG Texas red (TR) conjugate was purchased from Jackson ImmunoResearch Laboratories, West Grove, PA.

### Preparation of GPIIb mutant cDNA constructs

Platelet GPIIb mRNA of an Iranian-Jewish patient with GT bearing a deletion-insertion mutation in exon 25 was cloned into normal pGEM7-GPIIb (generously provided by Dr Peter Newman, Blood Center of South-eastern Milwaukee, WI) to create GPIIb-alt.25 as described previously.<sup>10</sup>

Platelet GPIIb mRNA was also prepared from an Iraqi-Jewish patient with GT who harbored a previously described splice-site mutation.<sup>11</sup> Approval was obtained from the Sheba Medical Center review board for these studies. Informed consent was provided according to the Declaration of Helsinki. Exons 13 to 22 were amplified by polymerase chain reaction (PCR) and cloned into a plasmid of the TA Cloning system (Invitrogen, San Diego, CA) and digested with *AccI* and *NruI* restriction enzymes. This yielded a cDNA fragment comprising nucleotides 1368 to 2198, which was used to replace the corresponding normal cDNA fragment of pGEM7-GPIIb, also digested with *AccI* and *NruI* restriction enzymes, to create GPIIb-del.20.

Full-length normal and mutated GPIIb cDNAs were excised from pGEM7 using *EcoRI* restriction enzyme. The cohesive ends were filled in with Klenow (Promega, Madison, MI) to create blunt ends and were subcloned into the *PvuII* site of pCEP4 mammalian expression vector carrying the hygromycin resistance gene as a selection marker (Invitrogen).

### Cell culture and cotransfection of GPIIb and GPIIIa cDNAs in baby hamster kidney (BHK) cells

BHK cells were grown in Dulbecco modified Eagle medium (DMEM) supplemented with 2 mg/mL L-glutamine and 5% fetal calf serum (Biological Industries, Beit-Haemek, Israel). The cells were transfected with 1  $\mu$ g pCDNA3-GPIIIa (generously provided by Dr D. L. French from Mount Sinai School of Medicine, New York, NY) using LipofectAMINE reagent (Gibco, Paisley, United Kingdom). The transfected cells were selected with medium containing 0.7 mg/mL G418 (Gibco). BHK cells resistant to G418 and stably expressing GPIIIa were transfected with 1  $\mu$ g of either normal or 1 of the 2 mutated forms of pCEP4-GPIIb using LipofectAMINE reagent. The transfected cells were selected with medium containing 0.7 mg/mL G418 and 0.5 mg/mL hygromycin (Boehringer Mannheim, Germany). Mock were cells expressing GPIIIa and transfected with 1  $\mu$ g pCEP4 (Invitrogen) and selected for resistance to both hygromycin and G418.

### Assessment of surface expression of GPIIb/IIIa complex by flow cytometry

Transfected cells were harvested with phosphate-buffered saline (PBS) and 5 mM EDTA [ethylenediaminetetraacetic acid], centrifuged, and incubated in growth medium for 30 minutes at room temperature. The cells were resuspended in PBS ( $5 \times 10^5$  cells per 100  $\mu$ L) and incubated with monoclonal antibodies against either GPIIb (SZ22, 15  $\mu$ g/mL), GPIIIa (AP3, 15  $\mu$ g/mL), or GPIIb/IIIa complex (10E5, 30  $\mu$ g/mL) for 30 minutes at room temperature. Cells were then washed with PBS, resuspended in 100  $\mu$ L PBS, and incubated for 30 minutes at room temperature with fluorescein isothiocyanate (FITC) conjugate goat antimouse IgG diluted 1:50. Finally, the cells were diluted to  $5 \times 10^4$ /mL, and surface fluorescence was analyzed in a Coulter flow cytometry (EPICS XL, Louton, United Kingdom).

### Immunoprecipitation of GPIIb and GPIIIa

BHK cells transfected with normal GPIIIa and either normal or mutant forms of GPIIb ( $5 \times 10^6$  cells) were lysed in lysis buffer (20 mM Tris [tris(hydroxymethyl)aminomethane] HCl [pH 7.5], 150 mM NaCl, 1% Nonidet P-40, 1% deoxycholic acid, and complete protease inhibitor mix [Boehringer Mannheim]). Cell lysates were incubated in ice for 30 minutes and centrifuged for 20 minutes at 16 000g to remove debris. The supernatant was incubated with 20  $\mu$ g rabbit polyclonal antibodies recognizing both GPIIb and GPIIIa or with 1  $\mu$ g CA3 monoclonal antibody against GPIIb overnight at 4°C followed by incubation with goat antirabbit IgG agarose or goat antimouse IgG agarose, respectively, for 5 hours at 4°C and then washed 5 times with TBST (20 mM Tris HCl [pH 7.5], 150 mM NaCl, 1% Triton X-100) and eluted at 100°C with reducing loading buffer (40 mM Tris [pH 6.8], 1.5% SDS, 8% glycerol, 0.01% bromophenol blue, and 5%  $\beta$ -mercaptoethanol). Immunoblot analyses were performed by 7.5% sodium dodecyl sulfate–polyacrylamide gel electrophoresis (SDS-PAGE), transfer to a polyvinylidene difluoride (PVDF) membrane (Millipore, Bedford, MA), and subjection to SZ22 monoclonal antibody against GPIIb followed by goat antimouse IgG peroxidase conjugate (Sigma). Immunoreactive bands on the membrane were detected using enhanced chemiluminescence (ECL) kit (Amersham, Buckinghamshire, United Kingdom) and x-ray film exposure. Prestained high molecular weight proteins (Bio-Rad Laboratories, Richmond, CA) were used to estimate the molecular weights of the precipitated proteins. In some experiments, immunoprecipitated proteins were treated with endoglycosidase H (New England Biolabs, Beverly, MA) as recommended by the manufacturer before the samples were analyzed on SDS-PAGE as described.

For immunoprecipitation of the GPIIb/IIIa complex, cells were lysed in the same lysis buffer but containing 5 mM CaCl<sub>2</sub>. The complex was precipitated either by 3  $\mu$ g P2 or 5  $\mu$ L rabbit antiserum against GPIIIa followed by adding IgG agarose conjugate antimouse or antirabbit antibody, respectively, and elution in sample buffer with or without 5%  $\beta$ -mercaptoethanol. Western blot analyses were performed using SZ22 and AP3 monoclonal antibodies followed by goat antimouse IgG peroxidase conjugate.

## Immunohistochemistry

Transfected BHK cells were grown on glass slides to subconfluence, washed in Tris-buffered saline (pH 7.6) with 5 mM CaCl<sub>2</sub> (TBS-Ca), dried for 24 hours at room temperature, and fixed in acetone for 15 minutes at 4°C. Cells were then incubated in TBS-Ca containing SZ22, AP2, or 10E5 monoclonal antibodies (10 to 20 μg/mL) using alkaline phosphatase-antialkaline phosphatase kit (APAAP, Dako, Glostrup, Denmark). Antibody binding to the cells was visualized as red staining using light microscopy and the Duet system (BioView, Rehovot, Israel).

## Immunofluorescence microscopy

Transfected cells were grown on 12-mm cover slips, washed in PBS, and fixed in acetone-methanol (1:1) as previously described.<sup>13</sup> Cells were incubated for 1 hour at room temperature with 1:1000 dilution of SZ22 monoclonal antibody against GPIIb, and either rabbit antirat mannosidase II or rabbit anticanine calnexin carboxyl terminus, followed by 1 hour of incubation with 1:70 FITC conjugate goat antimouse IgG or 1:40 TR conjugate goat antirabbit IgG, respectively. The cover slips were coated with antifade solution (Oncor, Gaithersburg, MD) and analyzed using the Duet system.

## Pulse-chase analysis

Transfected cells were metabolically labeled with [<sup>35</sup>S]methionine and chased for 1 to 24 hours as previously described.<sup>13</sup> Total GPIIb was immunoprecipitated from cell lysates with 3 μg SZ22 monoclonal antibody, and the GPIIb fraction complexed with GPIIIa was precipitated with AP3 or 10E5 antibodies. The immunoprecipitations were carried out at 4°C for 16 hours, which was followed by incubation with agarose-conjugated goat antimouse IgG (50 μL) for 5 hours at 4°C. Recombinant proteins without reducing agent were electrophoresed by SDS-PAGE, and the gel was fixed in isopropanol-acetic acid-water (25:10:65), vacuum dried, and exposed to Biomax MS film using Biomax Transcreen-LE (Kodak, Rochester, NY) at -70°C. Relative amounts of the separated proteins were estimated by densitometry (Clinscan2, Helena Laboratories, Beaumont, TX). In some experiments, immunoprecipitated proteins were treated with peptide N-glycosidase F (PNGaseF) (New England Biolabs) before they were subjected to SDS-PAGE.

## Molecular modeling of GPIIb

Because αIIb and α<sub>v</sub> are homologous proteins with 36% identity in amino acid sequence<sup>14</sup> and because αIIbβ3 (GPIIb/IIIa complex) and α<sub>v</sub>β3 share the same β3 subunit, we used the recently described crystal structure of human α<sub>v</sub>β3 (PDB:1JV2)<sup>7</sup> as a template for modeling β-propeller, calf-1, and calf-2 domains of GPIIb. Homology modeling was done separately for calf-1 and calf-2 domains in wild-type and in GPIIb-del.20 and GPIIb-alt.25 using Modeler of InsightII software (Accelrys, San Diego, CA). The Modeler performs automated homology modeling by simultaneously combining information from the sequence alignment and structures of multiple reference proteins.<sup>15</sup> The sequences of αIIb (XP\_045985), α<sub>v</sub> (XP\_002379), and α4 (XP\_039011) were aligned by Pileup algorithm (GCG, Accelrys). Normal and mutant GPIIb models and the α<sub>v</sub> template were superimposed by structure using the appropriate InsightII option. The amino acids of calf-1 and calf-2 domains of αIIb located in the interface with β3 subunit at 0.5 nm (5 Å) distance were marked and the nature of the contact analyzed using contacts of structural units (CSU) software.<sup>16</sup>

## Results

### GPIIb is formed but not surface expressed in cells transfected with GPIIb mutants

Fluorescence-activated cell sorter (FACS) analyses with monoclonal antibodies SZ22 and 10E5 recognizing GPIIb and GPIIb/IIIa, respectively, demonstrated lack of surface expression of GPIIb and

GPIIb/IIIa in cells transfected with alt.25 or del.20 mutations (Figure 1). Using AP3 monoclonal antibody against GPIIIa detected GPIIIa on the surface of cells containing normal as well as mutant GPIIb. This resulted from complex formation between human GPIIIa and hamster α<sub>v</sub>, as previously described.<sup>13,17</sup> Immunohistochemistry experiments using SZ22 antibody showed that expression of GPIIb occurred in cells transfected with normal GPIIIa and GPIIb-alt.25 (Figure 2). In cells containing the GPIIb-del.20 mutation, only weak staining with SZ22 was observed. These results indicate that the mutated forms of GPIIb were absent from the cell membrane but present intracellularly.

To further analyze the nature of the mutant forms of GPIIb, cell lysates were first immunoprecipitated with polyclonal antibody against GPIIb and GPIIIa and then subjected to SDS-PAGE with β-mercaptoethanol followed by Western blotting using SZ22 monoclonal antibody. Cells transfected with normal GPIIb displayed 2 bands corresponding to mature GPIIb and pro-GPIIb (Figure 3A). Cells transfected with GPIIb-alt.25 exhibited only one band, which migrated as pro-GPIIb, and cells transfected with GPIIb-del.20 exhibited a fast-migrating pro-GPIIb corresponding to the predicted deletion of 50 amino acids of exon 20 (Figure 3A). In these experiments the amount of both mutated GPIIb proteins, particularly GPIIb-del.20, was lower than the amount of wild-type (WT) GPIIb. When immunoprecipitation was carried out with a monoclonal antibody CA3 against GPIIb, and immunoblotting was performed with SZ22 monoclonal antibody, an additional smaller GPIIb-related band was observed in both GPIIb-alt.25 and GPIIb-del.20 (Figure 3B). These smaller bands probably represent *in vivo*-generated degraded GPIIb because cell lysates were prepared in the presence of protease inhibitor cocktail contained in the commercial tablets.

### GPIIb/IIIa complex is formed in cells expressing the GPIIb mutants

GPIIb/IIIa complex formation in cells expressing the GPIIb mutations was examined by immunostaining with 2 distinct monoclonal antibodies against the complex, 10E5 and AP2 (Figure 2). Compared with WT cells transfected with normal GPIIb, the cells transfected with GPIIb-alt.25 or GPIIb-del.20 reacted only faintly with 10E5 monoclonal antibody. Use of monoclonal antibody AP2 clearly showed the presence of the

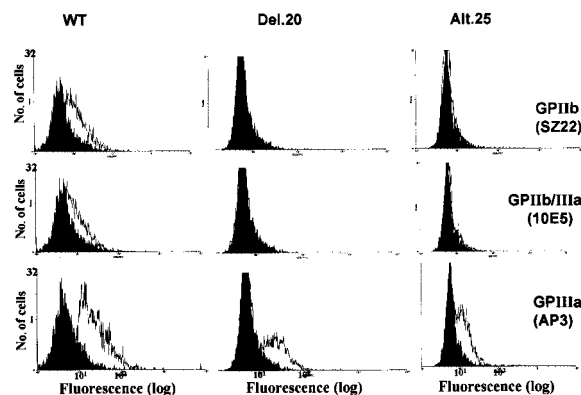
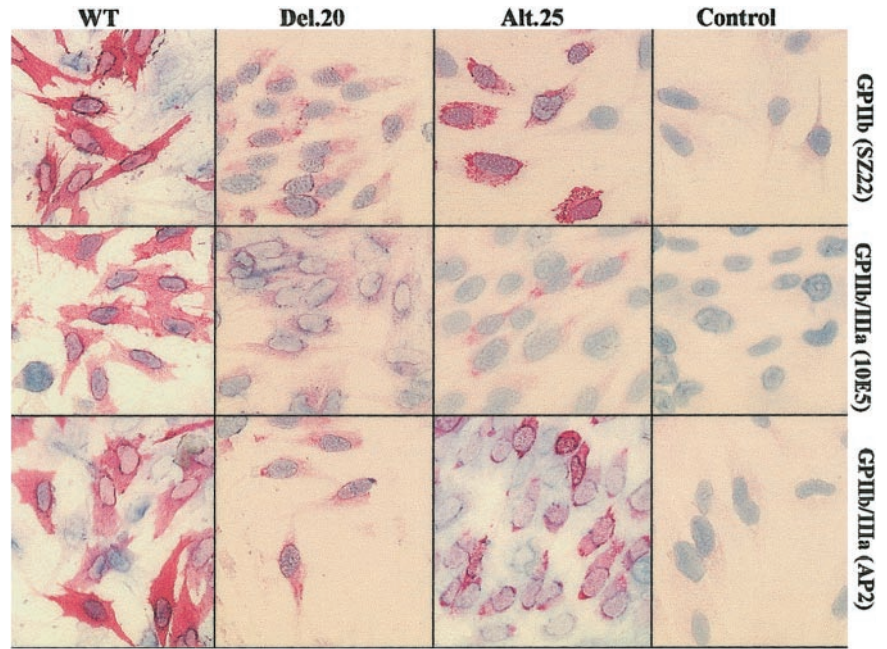


**Figure 1. FACS analysis of transfected cells.** Open histograms show the results from BHK cells expressing normal GPIIIa that were transfected with cDNA of normal GPIIb (WT) or mutated GPIIb (del.20 or alt.25). Monoclonal antibodies against GPIIb (SZ22), GPIIIa (AP3), and GPIIb/IIIa (10E5) were used. FITC-antimouse IgG plots are shown as black histograms. WT cells exhibited surface expression of GPIIb, GPIIIa, and GPIIb/IIIa, whereas cells containing GPIIb-del.20 or GPIIb-alt.25 displayed neither GPIIb nor GPIIb/IIIa but did display GPIIIa complexed with hamster α<sub>v</sub>.

**Figure 2. Immunostaining of transfected cells.** WT BHK cells transfected with normal GPIIIa and GPIIb cDNAs displayed immunostainable GPIIb and GPIIb/IIIa detected with monoclonal antibodies against GPIIb (SZ22) and GPIIb/IIIa (10E5 and AP2). Cells containing GPIIb-del.20 exhibited faint staining with the 3 antibodies, and GPIIb-alt.25 cells exhibited more conspicuous staining with AP2 and SZ22 but not with 10E5. Control BHK cells were transfected with GPIIIa cDNA and pCEP4. Original magnification,  $\times 200$ .



complex in cells transfected with GPIIb-alt.25 and less conspicuously in cells transfected with GPIIb-del.20.

To further analyze whether or not the mutants of GPIIb formed GPIIb/IIIa complexes, we examined the coprecipitation of mutants and normal GPIIb with GPIIIa using an antibody against GPIIIa. Cell lysates expressing each mutant of GPIIb (and normal GPIIIa) were first immunoprecipitated with polyclonal antibody against GPIIIa and then immunoblotted with a mixture of monoclonal antibodies SZ22 against GPIIb and AP3 against GPIIIa. Figure 4A-B shows that both GPIIIa and GPIIb were clearly demonstrable in reduced and nonreduced gels containing WT and the mutants of GPIIb. Notably, in nonreduced conditions, the SZ22 antibody similarly recognized WT GPIIb and the mutants of GPIIb (Figure 4B). Immunoprecipita-

tion of cell lysates with monoclonal antibody P2 recognizing GPIIb only when complexed with GPIIIa also revealed pro- and mature normal GPIIb, pro-GPIIb-alt.25, and a band corresponding to pro-GPIIb-del.20 (Figure 4C). Degraded GPIIb (Figure 3B) was absent in these gels. When GPIIb complexed with GPIIIa was precipitated by AP3 and analyzed with SZ22 in immunoblotting and long exposure, small amounts of mature GPIIb-alt.25 and a minute amount of mature GPIIb-del.20 were demonstrable (Figure 4D). Taken together, these experiments indicate that GPIIb/IIIa complexes are formed in cells harboring GPIIb-alt.25 and GPIIb-del.20.

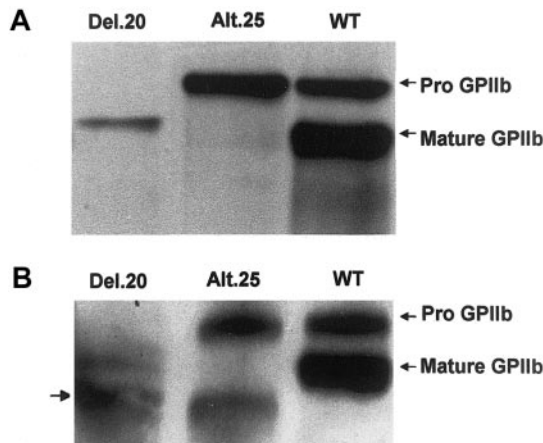


**Figure 3. Identification of mutant GPIIb in cells expressing del.20 and alt.25.** Shown are Western blots of immunoprecipitated GPIIb and GPIIIa from lysates of cells transfected with normal GPIIIa and normal or mutant GPIIb cDNAs. (A) Immunoprecipitation by polyclonal antibody against GPIIb and detection of GPIIb by SZ22 monoclonal antibody revealing both mature GPIIb and pro-GPIIb in WT cells, only pro-GPIIb in GPIIb-alt.25, and a fast-migrating pro-GPIIb in GPIIb-del.20. (B) Immunoprecipitation with CA3 monoclonal antibody against GPIIb followed by Western blot analysis with SZ22 revealing the same pattern as in panel A but an additional smaller band in the mutants probably representing a GPIIb degradation product.

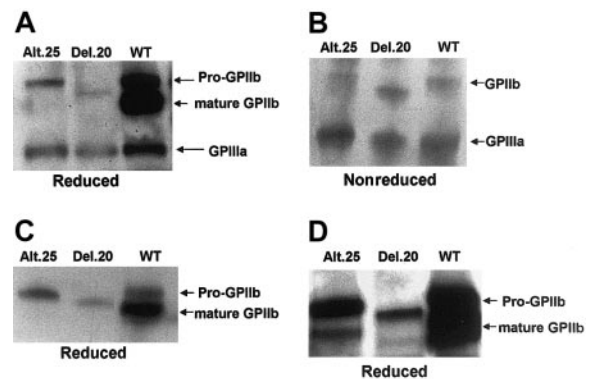


**Figure 4. Identification of the GPIIb/IIIa complex in cells expressing normal or mutant GPIIb.** GPIIIa was precipitated from lysates of normal or mutant-containing cells by polyclonal antibody against GPIIIa. Precipitates were subjected to SDS-polyacrylamide gels with (A) or without (B)  $\beta$ -mercaptoethanol, and Western blot analysis was carried out using monoclonal antibodies against GPIIb (SZ22) and GPIIIa (AP3) for detection of coprecipitated GPIIb with GPIIIa. (C) GPIIb/IIIa complex precipitated from lysates of normal or mutant-containing cells by monoclonal antibody P2 recognizing GPIIb only when complexed with GPIIIa, and subjected to SDS-polyacrylamide gel electrophoresis with  $\beta$ -mercaptoethanol. Western blots carried out with SZ22 show the same pattern as in panel A. (D) Coprecipitation of GPIIb with AP3 anti-GPIIIa monoclonal antibody analyzed in reduced gel by SZ22 monoclonal antibody. Overexposure of the gel detected a weak band corresponding to mature form of GPIIb in cells containing GPIIb-alt.25 and a faint band in cells containing GPIIb-del.20, which correspond to mature aberrant GPIIb.

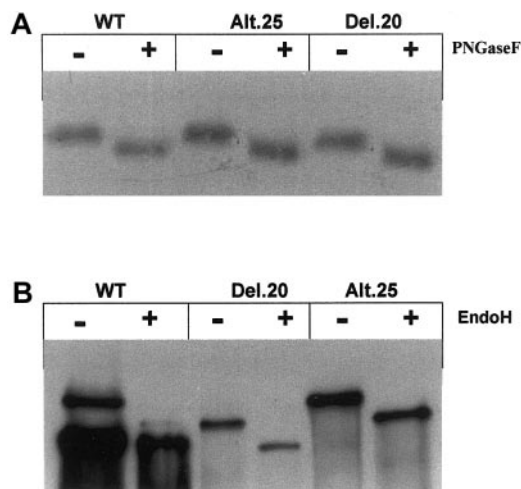


**Figure 5. Oligosaccharide processing.** (A) SDS-PAGE of <sup>35</sup>S-labeled GPIIb precipitated with SZ22 monoclonal antibody from cell lysates showing that PNGaseF acted similarly on lysates of cells containing normal and mutant GPIIb, indicating normal N-glycosylation. (B) Lysates of transfected cells containing normal or mutant GPIIb were precipitated by polyclonal antibodies against GPIIb and treated with EndoH. Shown is Western blot analysis using anti GPIIb antibody (SZ22) of SDS-PAGE in the presence of β-mercaptoethanol of cell lysates. Notable are resistance to EndoH for mature GPIIb in WT cells and sensitivity to EndoH for pro-GPIIb in cells containing GPIIb mutants as well as WT pro-GPIIb.

### Oligosaccharide processing of the mutated GPIIb

Because both mutants of GPIIb were produced in transfected cells and assembled as GPIIb/IIIa complex, we investigated the glycosylation of the GPIIb mutants. The initial stage of glycosylation, which takes place in the endoplasmic reticulum (ER), was examined by treatment of SZ22-immunoprecipitated cell lysates with peptide N-glycosidase F (PNGaseF), which cleaves the bonds between the innermost oligosaccharides and the asparagine in N-linked glycoproteins. Figure 5A shows that PNGaseF treatment resulted in the same changes in the migration of nonreduced GPIIb in WT, del.20, and alt.25 cells, indicating that both normal GPIIb and mutants of GPIIb underwent similar N-glycosylation. Complex N-glycosylation in the Golgi was assessed by resistance to endoglycosidase H (EndoH) digestion, which removes only non-complex N-mannose oligosaccharide chains in the ER. Figure 5B shows that while WT mature GPIIb was resistant to EndoH digestion (migration was similar), both mutants del.20 and alt.25 GPIIb were EndoH-sensitive similarly to WT pro-GPIIb as depicted by a change in their migration in reduced gel.

### Stability of the GPIIb mutants

To examine intracellular stability of the GPIIb mutants, cells harboring them were pulse labeled with [<sup>35</sup>S]methionine for 30 minutes and then lysed or chased with unlabeled methionine for 1 to 24 hours and then lysed. Total GPIIb was immunoprecipitated from cell lysates using SZ22. Figure 6A demonstrates that GPIIb levels in cells containing WT GPIIb decayed gradually and almost disappeared after 7 hours. GPIIb-alt.25 decayed slightly faster and GPIIb-del.20 decayed slightly slower than WT GPIIb. The generation and stability of the normal GPIIb/IIIa complex was examined by immunoprecipitation of the complex by 10E5 monoclonal antibody as described. Figure 6B demonstrates that the amount of normal GPIIb/IIIa increased during the first 2 hours and then declined. Because similar experiments with the mutants did not yield analyzable gels, probably due to diminished affinity of 10E5

to the mutated complexes, we precipitated the mutated complexes by AP3. The results showed that the GPIIb mutants complexed with GPIIIa and degraded in a pattern similar to WT complexes (Figure 6B). Collectively, these experiments suggest that mutant GPIIb/IIIa complexes formed and degraded at a rate that is similar to WT GPIIb/IIIa complex.

### Cellular localization of alt.25 and del.20 GPIIb mutants

To determine the cellular localization of GPIIb-alt.25 and GPIIb-del.20 mutants, immunofluorescence staining was performed using concomitantly SZ22 monoclonal antibody against GPIIb and rabbit polyclonal antibodies against calnexin (an ER marker) or SZ22 monoclonal antibody against GPIIb together with rabbit polyclonal antibodies against mannosidase II (a Golgi marker). Secondary antibodies used were antimouse FITC and antirabbit Texas red conjugates, which depict GPIIb in green, the ER or Golgi in red, and colocalization of GPIIb and the organelle markers in yellow. ER-calnexin distributed mainly around the nuclei (Figure 7A in red) while Golgi-mannosidase II was aggregated in clumps (Figure 7B in red). In WT transfected cells GPIIb was distributed evenly all over the cell, including the plasma membrane (Figure 7A in green), and a fraction colocalized with both calnexin and mannosidase II (yellow, Figure 7A and 7B, respectively). This suggested that some fraction of WT GPIIb could be found in the ER or the Golgi apparatus. In cells expressing the mutants GPIIb del.20 and alt.25, GPIIb (green) was distributed mainly around the nuclei as calnexin (Figure 7A, red and yellow) while the mannosidase II was aggregated in red clumps (Figure 7B). Only in 1 of 20 cells expressing GPIIb-alt.25 and in 1 of 25 cells expressing GPIIb-del.20 was a fraction of GPIIb colocalized with mannosidase II—that is, was present in the Golgi. These results fit with the finding of minute amounts of mature GPIIb in immunoprecipitation experiments (Figure 4D). Taken together, these data suggest that the mutants GPIIb-del.20 and alt.25 were localized mostly in the ER and only trace amounts reached the Golgi apparatus.

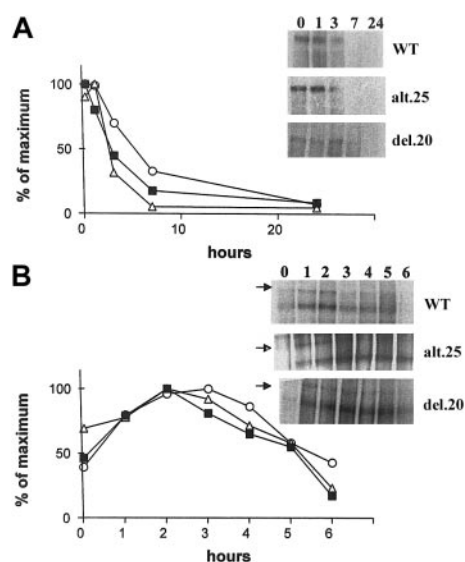
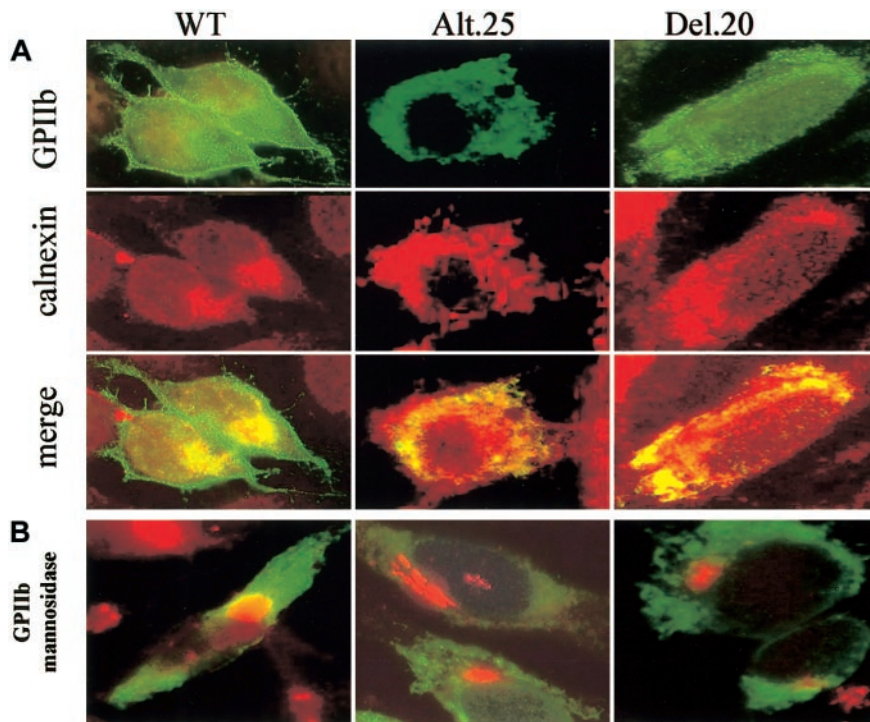


**Figure 6. Pulse-chase analysis of normal and GPIIb mutants.** Autoradiography of immunoprecipitated GPIIb pulse-labeled and chased with [<sup>35</sup>S]methionine and cold methionine, respectively. (A) Total GPIIb precipitated by SZ22 in the absence of CaCl<sub>2</sub>. (B) GPIIb complexed with GPIIIa precipitated in the presence of CaCl<sub>2</sub> by 10E5 for WT and by AP3 for GPIIb-alt.25 and GPIIb-del.20. The relative intensity of labeled bands was determined by densitometry and expressed as percent of maximum incorporation. ■ indicates WT; △, alt.25; and ○, del.20.

**Figure 7. Cellular localization of GPIIb by immunofluorescence staining.** (A) Transfected cells were stained simultaneously with SZ22 against GPIIb (green) and calnexin, an ER marker (red). The yellow color demonstrates colocalization of GPIIb with an organelle marker (merger of red and green). WT GPIIb is localized in the plasma membrane as well as the ER, whereas alt.25 and del.20 GPIIb are located only in the ER. (B) Transfected cells were stained simultaneously with SZ22 against GPIIb (green) and rabbit polyclonal antibodies against mannosidase II (red). Colocalization of GPIIb and mannosidase II, a Golgi marker, is seen in cells with WT GPIIb but not in cells harboring GPIIb alt.25 and del.20. Original magnification,  $\times 1000$ .



**The effects of the GPIIb mutants on the contact between GPIIb and GPIIIa**

The models of  $\beta$ -propeller, calf-1, and calf-2 domains of GPIIb were structurally superimposed with  $\beta$ -propeller, calf-1, and calf-2 domains of  $\alpha_v$ , and the contacts of the respective domains with  $\beta 3$  subunit seemed to be similar (Figure 8A). The crystal structure of  $\alpha_v\beta 3$  was originally resolved at a resolution of 0.31 nm (3.1Å),<sup>7</sup> which does not enable accurate determination of interatomic distances. Nevertheless, approximations of important interactions, which stabilize the structure of the complex and the size of the interface between  $\alpha_v$  and  $\beta 3$ , were calculated by CSU software.<sup>16</sup>

The size of the  $\alpha_v$   $\beta$ -propeller interface with  $\beta 3$  was the largest (24.28 nm<sup>2</sup>), whereas the sizes of the  $\alpha_v$  calf-1 and calf-2 interfaces with the  $\beta 3$  subunit were 2.74 nm<sup>2</sup> (9 amino acids) and 8.54 nm<sup>2</sup> (14 amino acids), respectively. Amino acid alignment of  $\alpha_v$  and  $\alpha$ IIb at the contact areas demonstrates that 3 of 9 amino acids were conserved in calf-1 and 5 of 14 amino acids were conserved in calf-2. None of the changes in the remaining amino acids was predicted to significantly hamper the contacts between calf-1 and calf-2 domains with the corresponding domains of  $\beta 3$ .

In the calf-1 domain of GPIIb-del.20, 50 amino acids are missing (Figure 8B, black), among which 3 take part in the contact

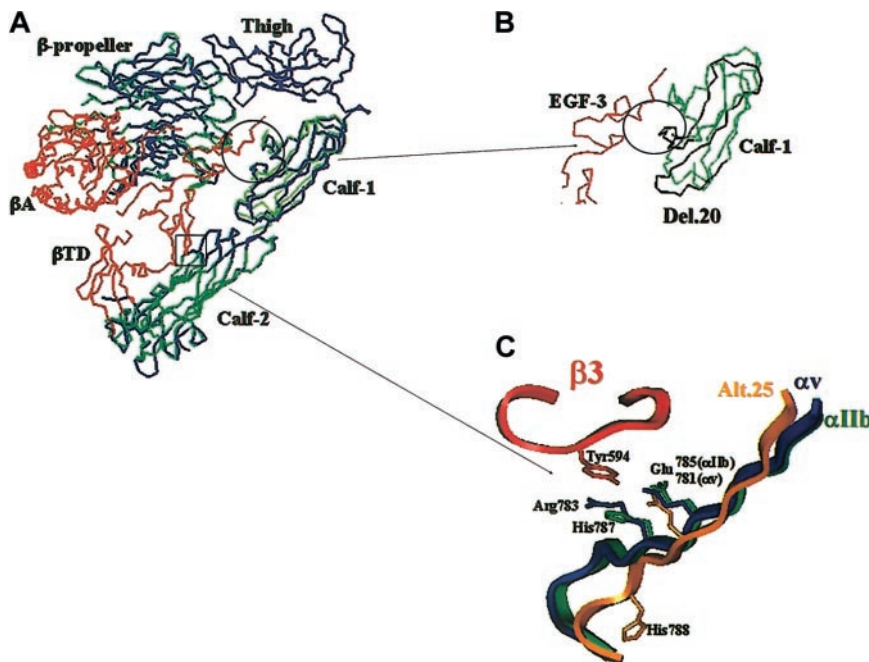


**Figure 8. Model structure of  $\alpha$ IIb superimposed on the crystal structure of  $\alpha_v\beta 3$ .** (A) Superimposition of  $\alpha_v\beta 3$  derived from the crystal structure (PDB:1jv2) and  $\alpha$ IIb derived from the predicted models of the  $\beta$ -propeller, calf-1, and calf-2 domains. The  $\alpha_v$  is shown in blue, GPIIIa ( $\beta 3$ ) in red, and GPIIb ( $\alpha$ IIb) in green. The interface between calf-1 and EGF-3 of  $\beta 3$  is circled, and the interface between calf-2 and EGF-4 of  $\beta 3$  is depicted in the square. (B) The interface between the calf-1 of GPIIb derived from the model and EGF-3 of GPIIIa derived from the crystal structure (red). The calf-2 backbone is shown in green and black; the black denotes the 50 amino acids deleted by del.20 mutation. The abolished contact with  $\beta 3$  is circled. (C) A region in the interface between  $\beta 3$  derived from the crystal structure (red) and calf-2  $\alpha_v$  derived from the crystal structure (blue) and  $\alpha$ IIb derived from the model (green) and  $\alpha$ IIb-alt.25 derived from model (gold). Notable is the profound displacement of His788 of GPIIb-alt.25; compare with His787 of normal GPIIb.

with  $\beta 3$  (1.64 nm<sup>2</sup>). Modeling of calf-1 of GPIIb-del.20 yielded a model with a score of 13.0, which is below the minimum score (17.8) for a correct protein of this size. Consequently, this model was not further analyzed. In the calf-2 domain of GPIIb-alt.25 the amino acid backbone is predicted to be shifted due to insertion of 8 amino acids replacing 10 amino acids of wild-type GPIIb. As a result of this shift, His788 was no longer in a position that allows contact with Tyr594 of  $\beta 3$ . Also, the distance between Glu785 and Tyr594 was increased in comparison with the normal interactions (Figure 8C). Hence, GPIIb-alt.25 is predicted to disrupt the contact of calf-2 domain with EGF-4 of  $\beta 3$  (1.47 nm<sup>2</sup>) but does not affect the other contacts with  $\beta$ TD.

## Discussion

The presented data show that 2 major mutations, GPIIb-del.20 and GPIIb-alt.25 in the calf-1 and calf-2 domains, respectively, enable GPIIb/IIIa complex formation but impair its transport from the ER to the Golgi apparatus, leading to absent surface expression of this complex. The mutants of GPIIb were detectable mostly as pro-GPIIb (Figures 3-5) and were localized mainly in the ER (Figure 7), findings that are consistent with conversion of pro-GPIIb to mature GPIIb in the Golgi apparatus.<sup>2</sup> Immunoprecipitation and pulse-chase experiments revealed that mutant GPIIb/IIIa complexes did form, although in apparently decreased amount, despite the markedly deranged GPIIb mutant proteins. The stability of the mutant proteins when complexed with normal GPIIIa appeared to be unimpaired (Figure 6). However, because of the limitation of pulse-chase experiments it cannot be ruled out that some degradation of GPIIb mutants occurred within the 30 minutes of the pulse (Figure 6). The presence of a GPIIb degradation product derived from the mutant proteins but not from normal GPIIb (Figure 3B) is consistent with such an assumption. Decreased amounts of mutant GPIIb proteins were also observed in immunostaining experiments (Figure 2) and immunoblotting analyses performed under reduced conditions (Figures 3, 4A,C-D, 5B) but not in immunofluorescence experiments (Figure 7) and immunoblotting analyses performed under nonreduced conditions (Figures 4B, 5A). Conceivably, variable recognition of the mutants of GPIIb by the antibodies under the different experimental conditions was responsible for the discrepant results. Together the data suggest that GPIIb-del.20 has a substantially greater negative effect on overall GPIIb synthesis than GPIIb-alt.25.

Other, albeit point mutations in the calf-2 domain, for example, Gln747Pro,<sup>18</sup> or in the calf-1 domain, for example, Cys674Arg,<sup>19</sup> were also associated with preserved intracellular complex formation yet with profoundly reduced surface expression. Moreover, major mutations in the calf-2 domain of GPIIb, for example, skipping of exon 28,<sup>20,21</sup> Ser870Stop,<sup>22</sup> and deletion of the whole GPIIb light chain,<sup>23</sup> were also shown to enable GPIIb/IIIa complex formation but impaired carbohydrate processing and surface expression of the complex. Finally, even a mutation associated with a deletion of both calf-1 and calf-2 domains (Arg597Stop) was recently found to enable formation of an unstable and rapidly

degradable GPIIb/IIIa complex.<sup>24</sup> Taken together, these observations suggest that significant changes in calf-1 or calf-2 domains do not prevent GPIIb/IIIa complex formation but do impair its transport to the cell surface, probably by its retention and degradation in the ER.

Our analysis of the  $\alpha_v\beta 3$  crystal structure and the predicted structure of  $\alpha$ Ib $\beta 3$  model showed that the main intersubunit contact between  $\alpha$ Ib and  $\beta 3$  subunit is the interface of the  $\beta$ -propeller of GPIIb and the  $\beta$ A domain of GPIIIa similar to what was described for the interface of  $\alpha_v$  and  $\beta 3$  in the  $\alpha_v\beta 3$  crystal. Disruptions of essential components in the  $\beta$ -propeller have consequently been shown to be associated with rapid degradation of the uncomplexed GPIIb mutants (del Ala106-Gln111, del Ser129-Ser161, Glu324Lys).<sup>25</sup> In contrast, missense mutations in the calcium-binding domain of the  $\beta$ -propeller, located away from the interface with  $\beta 3$ , Gly242Asp, Arg327His, Gly418Asp<sup>25</sup> were shown to enable GPIIb/IIIa complex formation but resulted in its retention in the ER. These observations indicate that the calcium-binding domain is also essential for the transport of the GPIIb/IIIa complex from the ER to the Golgi.<sup>25,26</sup>

Our analyses of the GPIIb/IIIa model that was based on the crystal structure of  $\alpha_v\beta 3$  showed that significant contacts exist between calf-1 of  $\alpha_v$  or  $\alpha$ Ib and EGF-3 of  $\beta 3$  and between calf-2 of  $\alpha_v$  or  $\alpha$ Ib and EGF-4 and  $\beta$ TD of  $\beta 3$ . Similar contacts between GPIIb and GPIIIa have also been shown by immunochemical methods<sup>6</sup> and by a recent electron microscopy study that involved physicochemical measurements.<sup>9</sup> In our analyses of the model, which are purely theoretical and unsupported by experimental data, the respective contacts were partially disrupted in mutant GPIIb-alt.25 and del.20. In GPIIb-alt.25 there was abolishment of the contact between amino group of Arg783 in  $\alpha_v$  or of His787 in  $\alpha$ Ib and the aromatic ring of Tyr594 in  $\beta 3$ , which is a known stabilizing structure,<sup>27,28</sup> and in GPIIb-del.20 there was a deletion of 3 amino acids that are in the contact area with  $\beta 3$  (Figure 8). Notwithstanding these significant disruptions, intracellular GPIIb/IIIa complex formation was formed and was stable. This supports the notion that the contacts between GPIIb and GPIIIa in the region of calf-1 and calf-2 domains are not essential for GPIIb/IIIa complex formation but apparently stabilize its bent conformation.<sup>9</sup> We speculate that the partial disruption of these contacts in del.20 and alt.25 mutants gives rise to conformational changes that are responsible for retention of the aberrant GPIIb/IIIa complex in the ER.

## Acknowledgments

We thank Dr Malka Reichart from Bioview and Maya Sokolovsky for their technical help with the visual computerized microscopy. We are grateful to the Bioinformatics Unit of the George S. Wise Faculty of Life Sciences at Tel Aviv University for providing technical assistance and computation facilities and to Barak Rotblat for his help with the protein modeling.

## References

- Phillips DR, Charo IF, Parise LV, Fitzgerald LA. The platelet membrane glycoprotein IIb-IIIa complex. *Blood*. 1988;71:831-843.
- Duperray A, Berthiere R, Chagnon E, et al. Biosynthesis and processing of platelet GPIIb-IIIa in human megakaryocytes. *J Cell Biol*. 1987;104:1665-1673.
- O'Toole TE, Loftus JC, Plow EF, Glass AA, Harper JR, Ginsberg MH. Efficient surface expression of platelet GPIIb-IIIa requires both subunits. *Blood*. 1989;74:14-18.
- Coller BS, Seligsohn U, Peretz H, Newman PJ. Glanzmann thrombasthenia: new insight from an historical perspective. *Semin Hematol*. 1994;31:301-311.
- French DL. Glanzmann thrombasthenia data-base. Available at: <http://med.mssm.edu/glanzmanndb>. Accessed June 1, 1999.
- Calvete JJ, Mann K, Alvarez MV, Lopez MM, Gonzalez-Rodriguez J. Proteolytic dissection of the isolated platelet fibrinogen receptor, integrin GPIIb/IIIa: localization of GPIIb and GPIIIa sequences putatively involved in the subunit interface and in intrasubunit and intrachain contacts. *Biochem J*. 1992;282:523-532.

7. Xiong JP, Stehle T, Diefenbach B, et al. Crystal structure of the extracellular segment of integrin  $\alpha\text{v}\beta 3$ . *Science*. 2001;294:339-345.
8. Weisel JW, Nagaswami C, Vilaire G, Bennett JS. Examination of the platelet membrane glycoprotein IIb-IIIa complex and its interaction with fibrinogen and other ligands by electron microscopy. *J Biol Chem*. 1992;267:16637-16643.
9. Takagi J, Petre BM, Walz T, Springer T. Global conformational rearrangements in integrin extracellular domains in outside-in and inside-out signaling. *Cell*. 2002;110:599-611.
10. Peretz H, Rosenberg N, Usher S, et al. Glanzmann's thrombasthenia associated with deletion-insertion and alternative splicing in the glycoprotein IIb gene. *Blood*. 1995;85:414-421.
11. Yatuv R, Rosenberg N, Dardik R, et al. Glanzmann thrombasthenia in two Iraqi-Jewish siblings is caused by a novel splice junction mutation in the glycoprotein IIb. *Blood Coagul Fibrinolysis*. 1998;9:285-288.
12. Dardik R, Kaufmann Y, Savion N, et al. Platelets mediate tumor cell adhesion to subendothelium under flow conditions: involvement of platelets GPIIb-IIIa and tumor cell  $\alpha\text{v}(\text{v})$  integrins. *Int J Cancer*. 1997;70:201-207.
13. Yatuv R, Rosenberg N, Zivelin A, et al. Identification of a region in glycoprotein IIIa involved in subunit association with glycoprotein IIb: further lessons from Iraqi-Jewish Glanzmann thrombasthenia. *Blood*. 2001;98:1063-1069.
14. Fitzgerald LA, Poncz M, Steiner B, Rall SC Jr, Bennett JS, Phillips DR. Comparison of cDNA-derived protein sequences of the human fibronectin and vitronectin receptor  $\alpha$ -subunits and platelet glycoprotein IIb. *Biochemistry*. 1987;26:8158-8165.
15. Braun W, Go N. Calculation of protein conformations by proton-proton distance constraints: a new efficient algorithm. *J Mol Biol*. 1985;186:611-626.
16. Sobolev V, Sorokina A, Prilusky J, Abola EE, Edelman M. Automated analysis of interatomic contacts in proteins. *Bioinformatics*. 1999;15:327-332.
17. Morel-Kopp MC, Kaplan C, Proulle V, et al. A three amino acid deletion in glycoprotein IIIa is responsible for type I Glanzmann's thrombasthenia: importance of residues Ile325Pro326Gly327 for  $\beta 3$  integrin subunit association. *Blood*. 1997;90:669-677.
18. Tadokoro S, Tomiyama Y, Honda S, et al. A Gln747Pro substitution in the  $\alpha\text{IIb}$  subunit is responsible for a moderate  $\alpha\text{IIb}\beta 3$  deficiency in Glanzmann thrombasthenia. *Blood*. 1998;92:2750-2758.
19. Gonzalez-Manchon C, Fernandez-Pinel M, Arias-Salgado EG, et al. Molecular genetic analysis of a compound heterozygote for the glycoprotein (GP) IIb gene associated with Glanzmann's thrombasthenia: disruption of the 674-687 disulfide bridge in GPIIb prevents surface exposure of GPIIb-IIIa complexes. *Blood*. 1999;93:866-875.
20. Kolodziej MA, Vilaire G, Rifat S, Poncz M, Bennett JS. Effect of deletion of glycoprotein IIb exon 28 on the expression of the platelet glycoprotein IIb/IIIa complex. *Blood*. 1991;78:2344-2353.
21. Iwamoto S, Nishiumi E, Kajii E, Ikemoto S. An exon 28 mutation resulting in alternative splicing of the glycoprotein IIb transcript and Glanzmann's thrombasthenia. *Blood*. 1994;83:1017-1023.
22. Vinciguerra C, Khelif A, Alemany M, et al. A nonsense mutation in the GPIIb heavy chain (Ser 870→stop) impairs platelet GPIIb-IIIa expression. *Br J Haematol*. 1996;95:399-407.
23. Frachet P, Duperray A, Delachanal E, Marguerie G. Role of the transmembrane and cytoplasmic domains in the assembly and surface exposure of the platelet integrin GPIIb/IIIa. *Biochemistry*. 1992;31:2408-2415.
24. Arias-Salgado EG, Tao J, Gonzalez-Manchon C, et al. Nonsense mutation in exon-19 of GPIIb associated with thrombasthenic phenotype: failure of GPIIb (597-1008) to form stable complexes with GPIIIa. *Thromb Haemost*. 2002;87:684-691.
25. French D. The molecular pathology of Glanzmann's thrombasthenia. In: Rao GHR, ed. *Handbook of Platelet Physiology and Pharmacology*. Boston, MA: Kluwer Academic Publishers; 1999: 394-423.
26. Calvete JJ. Clues for understanding the structure and function of a prototypic human integrin: the platelet glycoprotein IIb/IIIa complex. *Thromb Haemost*. 1994;72:1-15.
27. Burley S, Petsko G. Amino-aromatic interactions in proteins. *FEBS Lett*. 1986;203:139-143.
28. Zhu WL, Tan XJ, Puah CM, et al. How does ammonium interact with aromatic group? A density functional theory (DFT/B3LYP) investigation. *J Phys Chem*. 2000;104:9573-9580.